Eur. Phys. J. D **63**, 103–109 (2011)
DOI: 10.1140/epjd/e2011-10560-3

THE EUROPEAN PHYSICAL JOURNAL D

Regular Article

Electron impact excitation into the $3p^5 4p$ levels from the $3p^5 4s$ metastable levels of argon

G.F. Du, J. Jiang, and C.Z. Dong[a]

Key Laboratory of Atomic and Molecular Physics & Functional Materials of Gansu Province, College of Physics and Electronic Engineering, Northwest Normal University, Lanzhou 730070, P.R. China

Received 4 October 2010 / Received in final form 5 January 2011
Published online 9 June 2011 –

Abstract. Electron impact excitation cross sections of argon from the $3p^5 4s$ matastable states to the excited states of $3p^5 4p$ configuration were calculated by using the fully relativistic distorted wave method, based on the multi-configuration Dirac-Fock (MCDF) theory. The influence of electron correlation effects on cross sections were discussed in detail. For low energy impact, it is found that the electron correlation effects have a large influence on the cross sections and make the cross sections smaller. However, this influence become smaller with the increasing of incident electron energy. The present results are in good agreement with the experiments of Boffard et al. [Phys. Rev. A **59**, 2749 (1999)] in most cases.

1 Introduction

Electron impact excitation (EIE) of noble gases has gained a lot of attention in recent years because of their applications in various gaseous electronics. Argon holds a particular position among the inert gases owing to its both relatively higher content in the earth's atmosphere (it occupies the third place after nitrogen and oxygen) and frequent presence in various plasma media. For the metastable state of argon, the reaction ability becomes higher, the lifetimes is long and the EIE cross sections are large, the excitation of metastable state of argon is therefore especially important for the understanding and modeling of argon plasmas.

In the past few decades, because the experimental measurements are difficult when the initial and final states of target atom are both excited states, most investigations have concentrated on atomic processes from the ground state, including excitation [1–6], elastic scatting [7–10] and ionization [11–13]. Only a few researches have been devoted to electron impact excitation cross sections from the metastable states. On the experimental side, Baranov et al. [14] have studied the excitations from the $3p^5 4s$ levels into the levels of the $3p^5 4p$ configuration in an argon plasma afterglow. They obtained excitation rate coefficients as a function of the electron temperature in the range from 3000 to 11 000 K, and attempted to extract the magnitudes and energy dependencies of individual cross sections. Mityureva et al. [15] published their results for the stepwise excitation of the $3p^5 4s\,(J = 2)$ metastable level of argon into levels of the $3p^5 4p$ configuration in the energy range from onset 12 eV. Boffard et al. [16] employed two different sources of metastable atoms, and measured excitation cross sections into eight levels of $2p$ manifold at low electron energies, as well as excitation into three levels at energies up to 400 eV. However, the results of Boffard et al. are strikingly different with Baranov et al. and Mityureva et al. in both magnitude and shape as a function of collision energy. On the theoretical side, the total EIE cross sections from the metastable states of argon were calculated using the multistate semirelativistic Breit-Pauli R-matrix method by Bartschat and Zeman [17], the semirelativistic first-order distorted-wave (SRDW) and plane-wave Born approximation (PWBA) by Maloney et al. [18], the distorted-wave (DW) method by Dasgupta et al. [19], the relativistic distorted-wave (RDW) approximation by Srivastava et al. [20]. However, there are still some big discrepancies between these calculations and experiments [16].

The ground state of Ar is $1s^2 2s^2 2p^6 3s^2 3p^6$. The first excited configuration $3p^5 4s$ consists of four levels with total angular momentum J equals 0, 1, and 2. The two levels with $J = 1$ are short-lived resonance levels which can decay to the $J = 0$ ground state, whereas the two metastable levels with $3p^5 4s$ $(J = 0)$ and $3p^5 4s$ $(J = 2)$, which denote as $1s_3$ and $1s_5$, are dipole forbidden for decaying to the ground state. The next set of ten excited levels arises from $3p^5 4p$ configuration with J values ranging from 0 to 3. In Paschen's notation these levels are labeled as $2p_1$ through $2p_{10}$ from the highest energy to the lowest. As knows, argon and xenon have the similar energy level structure. In the previous work on electron impact excitation of Xe [21], we have studied the EIE

[a] e-mail: dongcz@nwnu.edu.cn

cross sections and energy levels from the metastable in detail. As an expansion of the study, a further calculation of the EIE cross sections for Ar has been performed in this work, the electron impact excitation cross section from the metastable states to the lowest excited states of $2p_1$ to $2p_{10}$ have been calculated systematically by a fully RDW program REIE06 developed by us [22,23], which is based on the multi-configuration Dirac-Fock (MCDF) method and the corresponding packages Grasp92 [24] and Ratip [25]. The influence of electron correlation effects on the cross section are also discussed in detail.

2 Theoretical method and calculational procedures

The electron impact excitation cross section $\sigma_{if}(\epsilon)$ from an initial state i to final state f can be written as [21,22,26,27]

$$\sigma_{if}(\varepsilon) = 8\frac{\pi a_0^2}{k_i^2 g_i}\sum_J (2J+1) \times \sum_{\kappa,\kappa'} |\langle \Psi_f | \sum_{p,qp<q}^{N+1} (V_{Coul} + V_{Breit}) | \Psi_i \rangle|^2 \quad (1)$$

where a_0 is the Bohr radius, k_i is the relativistic wave number of the incident electron, g_i is the statistical weight of the initial level of the N-electron target ion, κ and κ' are the relativistic quantum numbers of the initial and final continuum electrons, respectively. V_{Coul} is the Coulomb operator and V_{Breit} ia the Breit operator [28]. The wave function for both the initial and final states of the impact systems are the antisymmetric wave functions of the total $(N+1)$ electron system including the target ion plus a continuum electron, which can be written as [22,26]

$$\Psi = \frac{1}{(N+1)^{\frac{1}{2}}}\sum_{p=1}^{N+1}(-1)^{N+1-p} \times \sum_{M_t,m} C(J_t j M_t m; JM)\Phi_{\beta_t J_t}(x_p^{-1})u_{\kappa m\varepsilon}(x_p) \quad (2)$$

where C is the Clebsch-Gordon coefficient, J_t, j and J are the angular momentum quantum numbers of the target ion, continuum electron and the impact system, respectively; $\Phi_{\beta_t J_t}$ are the target-atom wave functions, β_t represents all other quantum numbers in addition to J_t; x_p designates the space and spin coordinates for electron p; and x_p^{-1} is the space and spin coordinates of the N electrons other than p; $u_{\kappa m\varepsilon}$ is the relativistic distorted-wave Dirac spinor for a continuum electron; κ is the relativistic quantum number. In our calculations, the continuum wave function $u_{\kappa m\varepsilon}(x_p)$ is generated by the component COWF and Ratip package [23,29] by solving the coupled Dirac equation in which the exchange effect between the bound and free electron is considered. The wave function $\Phi_{\beta_t J_t}(x_p^{-1})$ of the target states is generated by the widely used atomic structure package Grasp92 [24]. The continuum orbitals are solutions of the Dirac-Fock equations

$$\left(\frac{d}{dr}+\frac{\kappa}{r}\right)P_\kappa(r) - \left(2c - \frac{E}{c} + \frac{V(r)}{cr}\right)Q_\kappa(r) = -\frac{X^P(r)}{r} \quad (3)$$

$$\left(\frac{d}{dr}-\frac{\kappa}{r}\right)Q_\kappa(r) + \left(-\frac{E}{c} + \frac{V(r)}{cr}\right)P_\kappa(r) = \frac{X^Q(r)}{r}. \quad (4)$$

Here, c is the speed of light, P_κ and Q_κ refer to continuum orbitals. and E is the kinetic energy of the scattered electron. Direct and exchange potentials, $V(r)$ and $X(r)$; are given by Grant et al. [30]. These equations are solved by the method of outward integration.

To illustrate the electron correlation effects of the target states on the cross sections, two correlation models, named model A and B, are used to describe the target states in the calculations. Model A is the single configuration (SC) approximation, including the configurations $3s^23p^6$, $3s^23p^54s$ and $3s^23p^54p$ similar to the descriptions of Srivastava et al. [20]. While model B is the multi-configu-ration (MC) approximation, which includes the configurations $3s^23p^6$, $3s^23p^54s$, and $3s^23p^54p$, $3s^23p^53d$, $3s^23p^54d$, and $3s^23p^54f$. In our calculations, all the single electron orbitals including the core ($1s_{1/2}, 2s_{1/2}, 2p_{1/2}$ and $2p_{3/2}$) and peels ($3s_{1/2}, 3p_{1/2}, 3p_{3/2}, 4p_{1/2}$ and $4p_{3/2}$) are obtained by using an extended optimal level (EOL) method. To deal with the rearrangement of the valence orbitals, all the relative levels are divided into six groups according to their parity and total angular momenta, namely, two is for the metastable states with $J=2$ and $J=0$ of the $3p^54s$ configuration, and the other four groups are for the states with $J=0$, $J=1$, $J=2$ and $J=3$ of the $3p^54p$ configuration, respectively. Then these states were optimized independently. In addition, in model B, all virtual single excitations from the $3s_{1/2}$, $3p_{1/2}$, $3p_{3/2}$ shells into the unoccupied $3d_{3/2}$, $3d_{5/2}$, $4s_{1/2}$, $4p_{1/2}$, $4p_{3/2}$, $4d_{3/2}$, $4d_{5/2}$, $4f_{5/2}$ and $4f_{7/2}$ shells are incorporated by using the active space method [24]. The numbers of configuration state functions (CSFs) used in model B for different level groups are listed in Table 1.

In Table 2, the excitation energies from the $1s_5$ to $2p_1$−$2p_{10}$ calculated in model A and B are listed and compared with the theoretical results [20] and the available

Table 1. Number of CSFs in the expansion of the target state functions in model B and number of the levels are used in the optimization of the wave functions of the different symmetry. J^P is the total angular momenta and parity of the levels, NL is the number of the optimized level; NCSF is the number of CSFs.

Configurations	J^P	NL	NCSF
$3s^23p^54s + 3s^23p^53d + 3s^23p^54d$	2–	1	339
	0–	1	48
$3s^23p^54p + 3s^23p^54f$	0+	2	82
	1+	4	197
	2+	3	272
	3+	1	255

Table 2. Excitation energy (in eV) from $1s_5$ to $2p_1$−$2p_{10}$ calculated in two models and comparison with the theoretical results of Srivastava et al. [20] and the experimental results of Boffard et al. [16].

Configuration	J^P	Paschen	Ref. [20]	Model A	Model B	Exp. [16]
$3p^3_{3/2}4p_{3/2}$	1+	$2p_{10}$	1.201	1.209	1.261	1.359
$3p^3_{3/2}4p_{3/2}$	3+	$2p_9$	1.327	1.339	1.472	1.527
$3p^3_{3/2}4p_{1/2}$	2+	$2p_8$	1.342	1.354	1.457	1.547
$3p^3_{3/2}4p_{1/2}$	1+	$2p_7$	1.402	1.413	1.573	1.605
$3p^3_{3/2}4p_{3/2}$	2+	$2p_6$	1.414	1.426	1.638	1.624
$3p^3_{3/2}4p_{3/2}$	0+	$2p_5$	1.510	1.551	1.703	1.725
$3p^1_{1/2}4p_{1/2}$	1+	$2p_4$	1.539	1.552	1.696	1.735
$3p^1_{1/2}4p_{3/2}$	2+	$2p_3$	1.555	1.568	1.752	1.754
$3p^1_{1/2}4p_{3/2}$	1+	$2p_2$	1.581	1.594	1.755	1.779
$3p^1_{1/2}4p_{1/2}$	0+	$2p_1$	1.715	1.991	1.827	1.931

experiments [16]. In this table, we can obviously find that the results in model A are in good agreement with the results of Srivastava et al. [20]. But it has some large discrepancies with the experiments, and this model can only provide a primary estimate for the target states. Instead, the results in model B are in reasonable agreement with the experiments with maximal discrepancy less than 6%. From this comparison, it becomes clear that the model B can give a more accurate description for the corresponding target states.

3 Results and discussion

The excitations from the $1s_5$ level to the $3p^5 4p$ levels can be divided into two groups according to their parent terms. One is the core-preserving excitations, which include six levels denoted as $2p_5$ to $2p_{10}$. The other is the core-changing excitations, which include four levels denoted as $2p_1$ to $2p_4$.

In Figure 1, for the excitations from the $1s_5$ to the $2p_5$−$2p_{10}$ (Figs. 1a−1f, corresponding to the core-preserving excitations), our results in two correlation models are compared with the experimental values of Boffard et al. [16] and other calculations at low energy range. In order to ensure convergence, the maximal partial $\kappa = 50$ is included in our calculations. Firstly, as can be seen from Figure 1a, the excitation cross sections from the $1s_5$ to the $2p_5$, which is a dipole forbidden transition, is significantly smaller than the optically allowed ones compared with other excitations. Both the R-matrix results of Maloney et al. [18] and the results of distorted-wave by Dasgupta et al. [19] are in good agreement with the experimental results of Boffard et al. [16]. Although our results in model A and model B display a similar variational trend with the experiments, it is still smaller than the experiments. According to the explanation of Boffard et al. [16], the experimental results would include some important cascade contributions for this excitation. Secondly, for the excitations from the $1s_5$ to the $2p_6$, $2p_8$ and $2p_9$, of which the experimental results are available, it is found that the cross section varies very slowly with the increasing of incident electron energy. For the excitation from the $1s_5$ to the $2p_6$ (Fig. 1b), our results in model A are larger than the experimental values of Boffard et al. [16] and other calculations. However, the results in model B are in agreement with the experimental results of Boffard et al. [16] reasonably. For the excitation from the $1s_5$ to the $2p_8$ (Fig. 1d), no other theoretical results are available, our results in model A are larger than the experiments. However, the results in model B display a similar variational trend with the experiments. For the excitation from the $1s_5$ to the $2p_9$ (Fig. 1e), our results in model A, the distorted-wave results of Dasgupta et al. [19] and the results of semirelativistic distorted-wave with CIV3 wave function (SRDW-CIV3) of Maloney et al. [18] are much larger than the experiments [16]. The results in model B and the R-matrix results of Maloney et al. [18] are in good agreement with the experiments [16]. Finally, for the excitations from the $1s_5$ to the $2p_7$ and $2p_{10}$ (Figs. 1c and 1f), there are no published experimental data and other theoretical results. It is found that the results in model B are smaller than the results in model A. The cross sections decrease fast with the increasing of incident electron energy in model A, however, the cross sections decrease slowly with the increasing of incident electron energy in model B.

Figure 2 shows the EIE cross sections from the $1s_5$ to the $2p_4$−$2p_1$ (Figs. 2a−2d), corresponding to the core-changing excitations). As can be seen from Figure 2a, for the excitation to the $2p_4$, apparently, the results of the plane-wave Born approximation and the SRDW-CIV3 of Maloney et al. [18] are much larger than the experimental results. The distorted-wave results of Dasgupta et al. [19] are similar with the R-Matrix results of Maloney et al. [18]. Especially, the results of model A, model B and the Srivastava et al. [20] are in good agreement with the experimental values of Boffard et al. [16]. In Figure 2b, for the excitation to the $2p_3$, compared with the experiments, it can be seen that the results in model A, the results of relativistic distorted-wave of Srivastava et al. [20] and the results of distorted-wave of Dasgupta et al. [19] show a similar variational trend with the experiments, but there are still big discrepancies compared with the experiments. However, our results in model B are in agreement with the experimental values of Boffard et al. [16]. In Figure 2c,

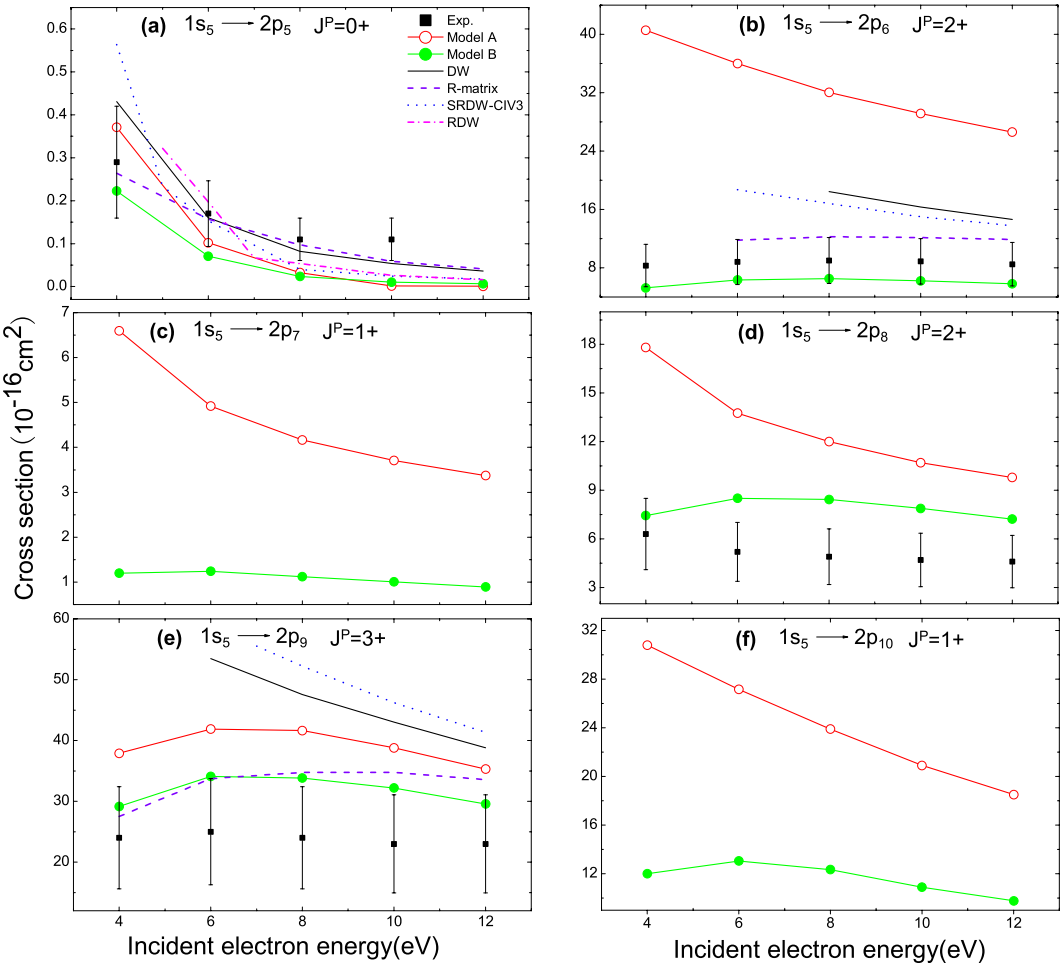

Fig. 1. (Color online) Electron impact excitation cross sections of argon. The hollow circles are the present results in model A; the solid hollow circles are the present results in model B; the solid line are the distorted-wave (D-W) results of Dasgupta et al. [19]; the dash line are the results of 15-states R-matrix of Maloney et al. [18]; the dot line are the results of SRDW with CIV3 wave functions (SRDW-CIV3) of Maloney et al. [18]; the dash-dot line are the RDW results of Srivastava et al. [20]; the squares with the error bars are the experiments of Boffard et al. [16].

there is also no other theoretical calculations, although our results in model B are smaller than that in model A, there are still about a factor of two larger than the experimental results of Boffard et al. [16], the reason mainly due to the incomplete inclusion of the correlation effects in the same model for $2p_2$. From Figure 2d, for the excitation from the $1s_5$ to the $2p_1$, obviously, it shows a similar variation trend with the excitation from the $1s_5$ to the $2p_5$ (Fig. 1a). And we can see the core-changing transitions have smaller cross sections compared with the core-preserving transitions.

In Figure 3, we carried out similar calculations for the excitations from the $1s_3$ to the $2p_1-2p_8$, $2p_{10}$ (Figs. 3a–3i) in two models, and compared with other theoretical calculations and available experiments of Boffard et al. [16]. It is found that for the excitations from the $1s_3$ to the $2p_1$, $2p_3$, $2p_5$, $2p_6$ and $2p_8$ (Figs. 3a, 3c, 3e, 3f and 3h), which are dipole forbidden transitions, and show a similar variational trend with the excitation from the $1s_5$ to the $2p_5$, the cross sections decrease rapidly with the increasing of incident electron energy. There is no available experimental data and theoretical result can be used to compare. The dipole allowed transitions which included the excitations from the $1s_3$ to the $2p_2$, $2p_4$, $2p_7$ and $2p_{10}$ (Figs. 3b, 3d, 3g and 3i), both the theory and experiment show a similar variational trend, that is, they have larger cross sections and decrease very slowly with increasing of incident electron energy. For the excitation from the $1s_3$ to the $2p_2$, there is also no other theoretical results to compare, it is found that our results in model B are still bigger than the experiments of Boffard et al. [16]. For the excitation from the $1s_3$ to the $2p_4$, compared with the available experiments and other theoretical results, it is found that our results in model B are smaller than those in model A, however, there have also some differences with the experiments and the results of R-matrix of Maloney et al. [18].

In the above sections, we compared our results with experimental values of Boffard et al. [16] and discussed the influence of electron correlation effects on cross sections at low energy range in detail. In Figure 4, further calculations

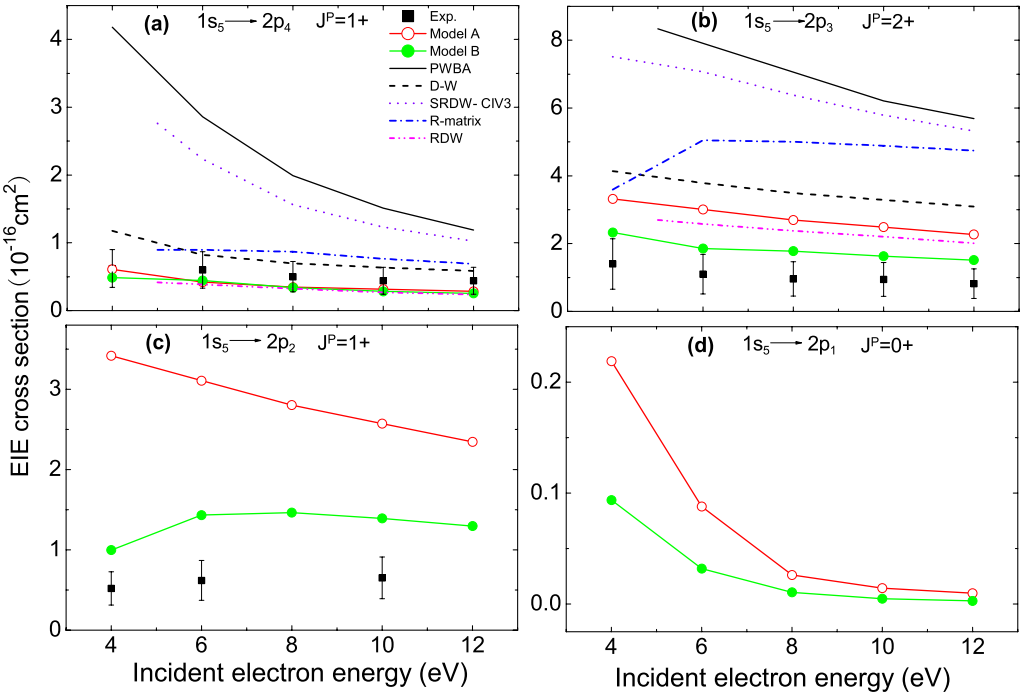

Fig. 2. (Color online) Electron impact excitation cross sections of argon. The hollow circles are the present results in model A; the solid hollow circles are the present results in model B. The solid line are the plane-wave Born approximations (PWBA) results of Maloney et al. [18]; the dash line are the distorted-wave (D-W) results of Dasgupta et al. [19]; the dot line are the SRDW-CIV3 results of Maloney et al. [18]; the dash-dot line are the results of 15-states R-matrix of Maloney et al. [18]; the dash-dot-dot line are the results of RDW results of Srivastava et al. [20]; the squares with the error bars are the experiments of Boffard et al. [16].

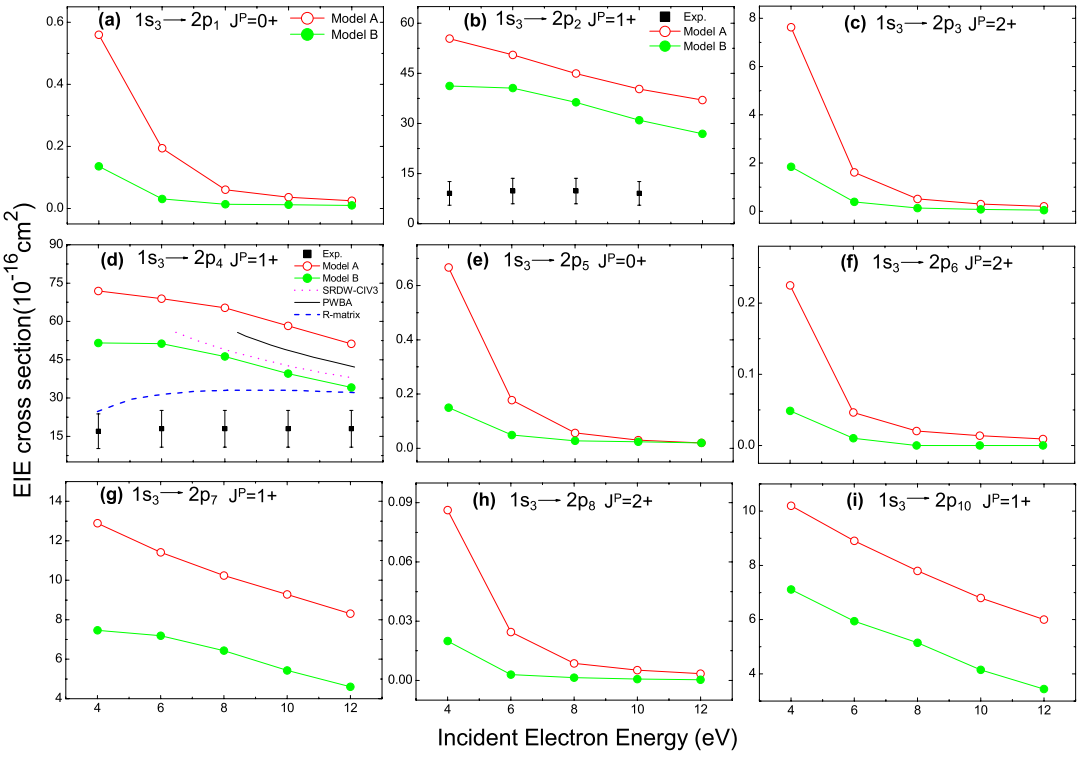

Fig. 3. (Color online) Electron impact excitation cross sections of argon. The hollow circles are the present results in model A; the solid hollow circles are the present results in model B. The solid line are the plane-wave Born approximations (PWBA) results of Maloney et al. [18]; the dash line are the results of 15-states R-matrix of Maloney et al. [18]; the dot line are the SRDW-CIV3 results of Maloney et al. [18]; the squares with the error bars are the experiments of Boffard et al. [16].

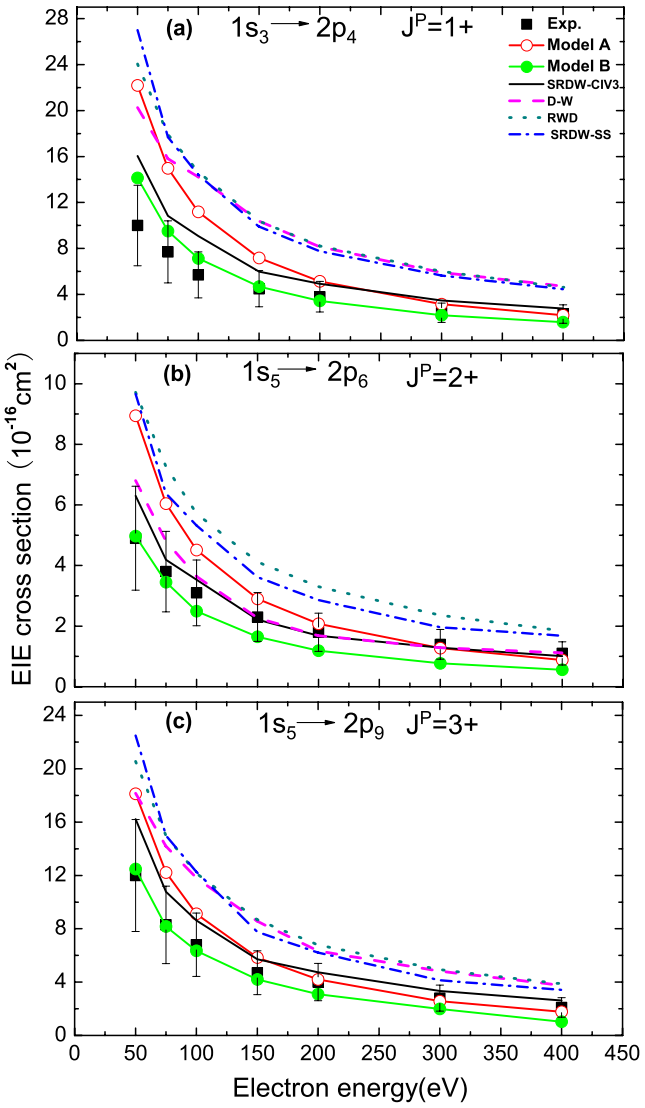

Fig. 4. (Color online) Electron impact excitation cross sections of argon. The hollow circles are the present results in model A, the solid circles are the present results in model B. The solid line are the SRDW-CIV3 results of Maloney et al. [18]; The dash line are the distorted-wave (D-W) results of Dasgupta et al. [19]; the dot line are the RDW results of Srivastava et al. [20]; the dash dot line are the SRDW results with SUPERSTRUCTURE program (SRDW-SS) of Maloney et al. [18]; the squares with the error bars are the experiments of Boffard et al. [16].

were carried out for these EIE cross sections for the energy range from 50 eV to 400 eV. Considering the importance of the high partial wave contribution in high energy impact, the maximal partial wave $\kappa = 180$ is included in the calculations. It is clearly found that our results in model A show a similar variational trend with the experiments of Boffard et al. [16]. However, both our results in model B and the SRDW-CIV3 results of Maloney et al. [18] are in good agreement with the experiments. With increasing of the incident electron energy, the results of distorted-wave of Dasgupta et al. [19], relativistic distorted-wave approximation of Srivastava et al. [20] and semirelativistic distorted-wave with SUPERSTRUCTURE (SRDW-SS) program of Maloney et al. [18] are consistent with the experiments results of Boffard et al. [16] gradually. Obviously, the EIE cross sections for high energy collision are not sensitive to description of the target states.

4 Conclusions

The RDW method is used to calculate the electron impact excitation cross sections of argon from the metastable states of the $3p^5 4s$ configuration to the states of the $3p^5 4p$ configuration. With the aim of getting more accurate target states, two different correlation models are used to describe the target states. From this work, we can conclude that correlation effects made the cross sections becomes smaller, at low energy region, both of the core-preserving excitation cross sections and core-changing excitation cross sections are very sensitive to the description of the target states. However, with increasing of the incident electron energy, the cross sections are not sensitive to the description of the target states. In most cases, our results in model B are in good agreement with the experiments of Boffard et al. [16].

This work was supported by the National Nature Science Foundation of China (Grant Nos. 10774122, 10876028, 10847007, 10964010) and the specialized Research Fund for the Doctoral Program of Higher Education of China (Grant No. 20070736001).

References

1. A. Chutjian, D.C. Cartwright, Phys. Rev. A **23**, 5 (1981)
2. R.S. Schappe, M.B. Schulman, L.W. Anderson, C.C. Lin, Phys. Rev. A **50**, 1 (1994)
3. S. Tsurubuchi, T. Miyazaki, K. Motohashi, J. Phys. B At. Mol. Opt. Phys. **29**, 1785 (1996)
4. S. Kaur, R. Srivastava, R.P. McEachran, A.D. Stauffer, J. Phys. B At. Mol. Opt. Phys. **31**, 873 (1998)
5. D.H. Madison, C.M. Maloney, J.B. Wang, J. Phys. B At. Mol. Opt. Phys. **31**, 4833 (1998)
6. R.K. Gangwar, L. Sharma, R. Srivastava, A.D. Stauffer, Phys. Rev. A **81**, 052707 (2010)
7. R.P. McEachran, A.D. Stauffer, J. Phys. B **16**, 4023 (1983)
8. D.E. Golden, H.W. Bandel, Phys. Rev. **149**, 1 (1966)
9. W.E. Kauppila, T.S. Stein, J.H. Smart, M.S. Dababneh, Y.K. Ho, J.P. Downing, V. Pol, Phys. Rev. A **24**, 2 (1981)
10. R.W. Wagenaar, F.J. de Heer, J. Phys. B **18**, 2021 (1985)
11. W. Lotz, Z. Phys. **206**, 205 (1967)
12. H.A. Hyman, Phys. Rev. A **20**, 3 (1979)
13. R.S. Freund, R.C. Wetzel, R.J. Shul, T.R. Hayes, Phys. Rev. A **41**, 7 (1990)
14. I.Yu. Baranov, N.B. Kolokolov, N.P. Penkin, Opt. Spektrosk. **58**, 268 (1985) [Opt. Spectrosc. **58**, 160 (1985)]

15. A.A. Mityureva, N.P. Penkin, V.V. Smirnov, Opt. Spektrosk. **66**, 790 (1989) [Opt. Spectrosc. **66**, 463 (1989)]
16. J.B. Boffard, G.A. Piech, M.F. Gehrke, L.W. Anderson, C.C. Lin, Phys. Rev. A **59**, 2749 (1999)
17. K. Bartschat, V. Zeman, Phys. Rev. A **59**, R2552 (1999)
18. C.M. Maloney, J.L. Peacher, K. Bartschat, D.H. Madison, Phys. Rev. A **61**, 022701 (2000)
19. A. Dasgupta, M. Blaha, J.L. Giuliani, Phys. Rev. A **61**, 012703 (2000)
20. R. Srivastava, A.D. Stauffer, L. Sharma, Phys. Rev. A **74**, 012715 (2006)
21. J. Jiang, C.-Z. Dong, L.-Y. Xie, X.-X. Zhou, J. Phys. B At. Mol. Opt. Phys. **41**, 245204 (2008)
22. J. Jiang, C.Z. Dong, L.Y. Xie, J.G. Wang, J. Yan, S. Fritzsche, Chin. Phys. Lett. **24**, 691 (2007)
23. J. Jiang, C.Z. Dong, L.Y. Xie, J.G. Wang, Phys. Rev. A **78**, 022709 (2008)
24. F.A. Parpia, C.F. Fischer, I.P. Grant, Comput. Phys. Commun. **94**, 249 (1996)
25. S. Fritzsche et al., Nucl. Instr. Methods B **205**, 93 (2003)
26. H.L. Zhang, D.H. Sampson, Phys. Rev. A **41**, 198 (1990)
27. J.F. Christopher et al., Phys. Rev. A **47**, 1009 (1993)
28. C.Z. Dong, S. Fritzsche, Phys. Rev. A **72**, 012507 (2005)
29. S. Fritzsche, J. Electron. Spectros. Relat. Phenomena **114–116**, 1155 (2001)
30. I.P. Grant et al., Comput. Phys. Commun. **21**, 207 (1980)